

Plasma, Polymerization of Ethane and Some Properties of PP Ethane as a Protective Coat

GUNERI AKOVALI, *Department of Chemistry and Macromolecular Research Division (TUMKA), Middle East Technical University, Ankara, Turkey*

Synopsis

The structure of plasma polymers of ethane prepared by use of 13.56 MHz radiofrequency discharge in a tubular reactor are examined. The dependency of rate of deposition on power and on tube pressure at a fixed flow rate are presented. The plasma polymer prepared is tested for its performance as a protective coat on NaCl optical components for use in CO₂ laser windows. Absorbance, at and around 10.6 μm , water-vapor transmission, and scratch-resistance tests are done.

INTRODUCTION

There is considerable interest and literature on plasma polymerization (PP) in a low temperature glow discharge.¹⁻³ Most of the work done are studies in gas phase which usually leads to amorphous and cross-linked films, in addition to those initiated in the liquid and solid states^{2,4,5} where the products are soluble.

For almost a decade, there has been a search for suitable protective coats for optical materials including components (i.e., filters, windows). For the latter, alkali metal halides are usually used in a large variety of environments; such as for laser detections and communication to satellite surveillance devices where protection from both atmosphere and other deterioration (i.e., micrometeorites) is needed. For infrared (IR) laser windows, the usual ranges sought are either at 10 μm and/or at 2-5 μm (for tunable lasers). The first of these (to be more specific, 10.6 μm) is the most popular for CO₂ lasers.⁶ Hence, the coat is expected to have nil or minimal intrinsic absorption at these wavelengths, with low water-vapor permeation, good adhesion, optimum antireflection characteristics, and uniform thicknesses up to $\lambda/40$ of the laser wavelength. In this study, PP ethane is tested to check its potential as a protective coat for NaCl crystals for use in laser systems.

For PP in gas phase, it is known that; in addition to a number of physical and electrical parameters, several operational parameters such as monomer flow rate-reactor tube pressure and power are of prime importance to consider for rate of PP deposition,⁷ for composition of the effluent gas within the plasma, and deposition rate profile.⁸ In this study, chemical characteristics of the deposit as a function of axial positions in the reactor as well as its aging characteristics are presented which supplements the author's previous publication,⁷ with the hope of shedding some more light on the subject.

EXPERIMENTAL

A plug-flow reactor (with pyrex walls and brass end plates) containing copper electrodes capacitively coupled to radiofrequency (rf) (13.56 MHz) is used. Teflon inserts are placed before and after the electrodes to form a gas passage of uniform cross-section. An IPC-Model PM401 generator is used. Details of the system were presented in another communication.⁷ Either "aluminium foil" or "NaCl optic crystals" are used, depending on the need, which are either placed on the cooled-grounded or on both electrodes. The surface of aluminium substrate is cleaned carefully with acetone and it is allowed to dry before the plasma process. The IR spectra are taken from crystal (or) KBr pellet with PE177 spectrometer. The rate of polymer deposition is determined by weighing pieces of aluminium foil, which was shown to yield the same result obtained with optical density and absorbance measurement⁷ and the maximum error estimated is 10%.⁹

Ethane used was obtained from Mattheson Gas Co. (CP grade). Environmental tests are done in a controlled humidity chamber with relative humidity of 88.8% produced by using proper mixtures of distilled water with H₂SO₄.¹⁰ Humidity resistance tests are done by exposing optical crystals (which are created on both sides by PP) to the atmosphere of the chamber for certain periods of time and then by examining their surfaces by optical microscopy. Some tests are repeated by leaving samples at room humidity for (standard) 100 hours. The extent of adherence of the film to the substrate surface is tested by "scratch test," which is shown to produce the most practical and reasonably consistent results compared with conventional "scotch tape" and "tip" tests.¹¹ In the tester, a smoothly rounded point is used which is drawn across the film surface. A vertical load is applied to the system until the film is stripped, and the applied load is used as a measure of the adhesion of the film (Fig. 1). In this work, the estimates of relative adhesion were obtained by comparison. Only a small portion of film is removed by this technique, and many additional scratch tests can be performed on the same sample without risking the probability of inhomogeneity of film thicknesses for different samples. The tester uses a tungsten carbide contact point such as a stylus, mounted on a balanced arm which has a pen for adding weights as the load. The sample is mounted on a movable stage and drawn slowly under the stylus, while the scratch tester is viewed from above with a microscope ($\times 100$). The sample is illuminated from below, thus the extent of film removal is easily seen as the light passes through the transparent substrate.

RESULTS AND DISCUSSION

To supplement earlier results,⁷ first a series of higher rf power levels are applied and the characteristic map obtained (Fig. 2) is found to consist of only film and powdery products as before; no oily polymer is traced out as reported by Jensen et al.⁸ Whether this discrepancy is due to the differences in reactor materials used in two systems (Lucite in the latter versus Pyrex in our case) or not is not clear yet and is under current investigation. The map presented here is consistent with the previous one and the effect of

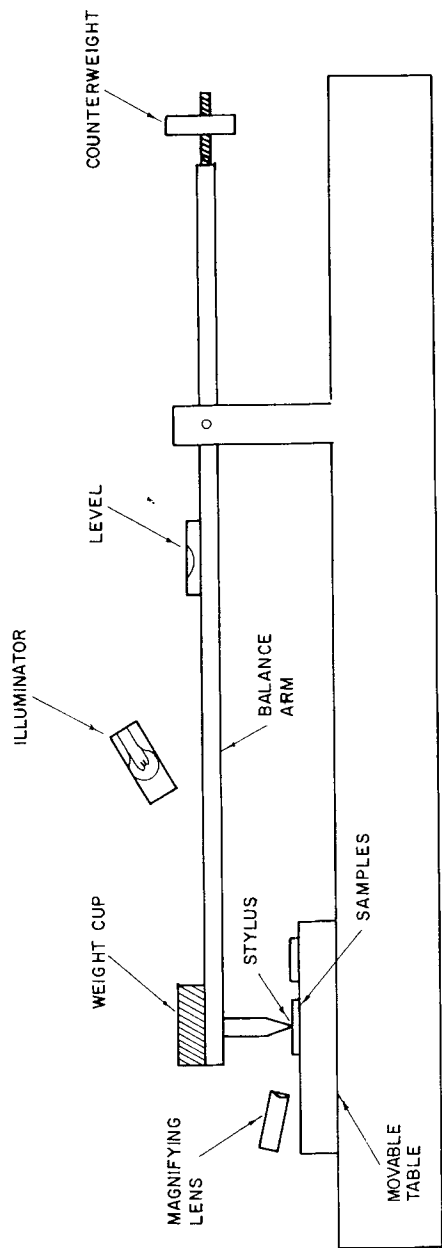


Fig. 1. Scratch-resistance tester (schematic).

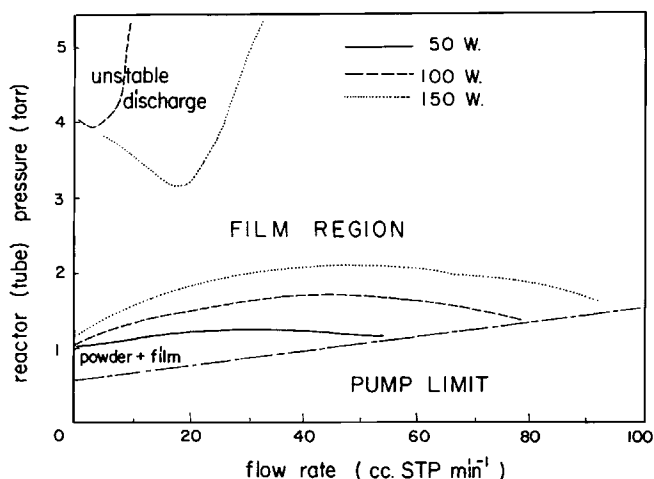


Fig. 2. Characteristic map of PPE.

increase of power seems to increase both (powder + film) and (unstable discharge) regions. Decrease in tube pressure and monomer flow rate enhances powder formation and at moderately higher pressures within a larger region, film PP ethane (PPE) is produced. As suggested before,⁷ powder is favored if polymerization is rapid which is expected to increase with the power dissipated.

The amount of film PPE deposited per unit substrate area versus plasma durations is plotted in (Fig. 3) for different selected tube pressures, all at 40 cc STP-min. constant monomer feed rate. The increase of power apparently increases both the amount of polymer deposited (per given area) as well as the rate of deposition (slope of the lines); whereas an inverse relationship is seen between pressure and deposition. The interrelations between deposition rate-*rf* power and pressure for the conditions studied is reproduced and presented in (Fig. 4). The increase of deposition rate with power is even more pronounced above 100 W. In the literature, there are several conflicting results in relation to power dependency of deposition rates. Although the result of Vasile and Smolinsky¹² for vinyl trimethyl silane and Thompson and Smolinsky¹³ for hexamethyl disiloxane in a bell jar reactor are similar to that observed here; previous findings of the author¹⁴ as well as studies of Yasuda¹⁵ and Hirotsuka et al.⁷ for same and different monomers yielded either inverse relationship or an increase followed by a decrease. The inconsistency most probably is due to the differences in monomers and in flow rates used. The response at very high or low flow rates is expected to be quite different than at intermediate.⁷ In fact, the increase in rate of deposition with input power can be easily explained by an increase in electron temperature and (number) density.

To follow chemical characteristics of PP film as a function of its axial position on the electrode a number of rectangular-polished NaCl optic crystals are placed on the cooled electrode one next to the other beginning from the inlet of the reactor. They are classified as T(T_1, T_2, \dots) and E(E_1, E_2, \dots)

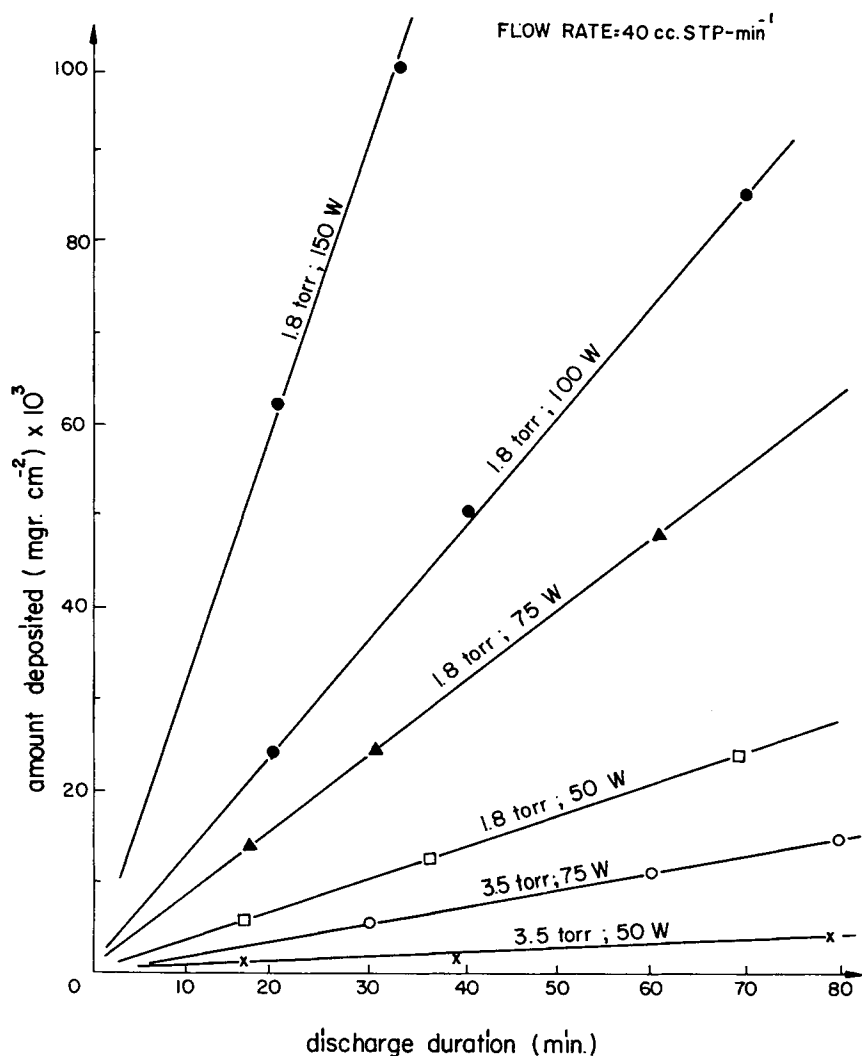


Fig. 3. Amount of deposition versus discharge duration curves for PPE at various reactor pressure and power levels. Flow rate of ethane: 40 cc STP/min.

to show whether they are on Teflon insert or on cooled electrode surface. Fig. 5 present a series of IR absorption spectra of PPE prepared at 1 Torr, 100 W, and 3.5 cc STP/min; for tube pressure, power, and monomer flow rate, respectively. It is clear that PPE samples obtained under the conditions studied have the same chemical structure being irrespective of its location; although the amount deposited may show some variations as notable from the differences in intensities of absorption bands, which most probably is due to differences in deposition rates. This point is further checked and deposition rate profiles at several pressure and flow rate levels are presented in Fig. 6. Although, profiles presented here are restricted only to plasma (electrode) region, they still show the tendency of increase in deposition rate

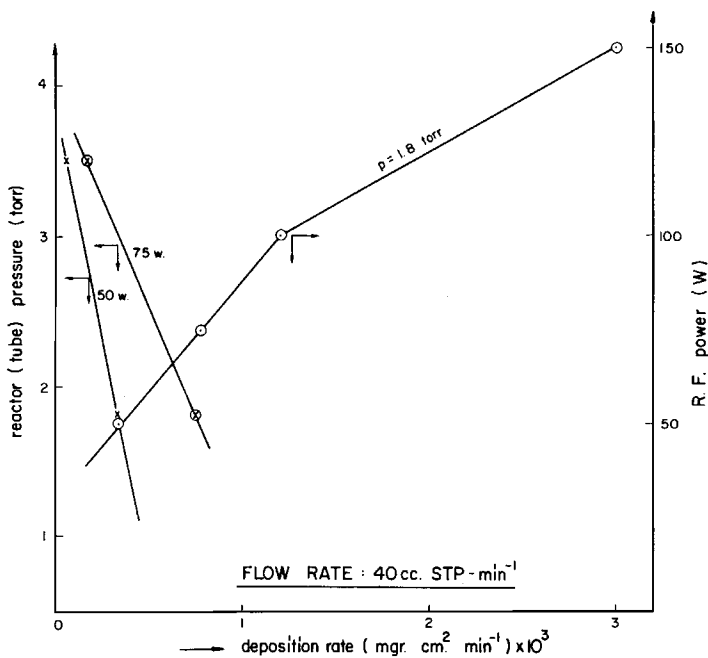


Fig. 4. Reactor tube pressure and rf power versus deposition rate plots for PPE. Flow rate of ethane: 40 cc STP/min.

from inlet edge of cooled electrode toward the outlet; which fits to the tendency presented by Jensen et al.⁸ However, one should also note that there is about an order of magnitude difference between the two data, which is larger in our work. Whether this difference can be attributed to differences in wall materials (Lucite, in Jensen et al.'s and Pyrex in this study) or not, is not clear at this stage.

PPE samples are checked for their radical activities (simply by letting them stand in atmosphere in dark for certain periods of time) by IR, and considerable increases in (OH) and (C-O) absorption peak intensities are observed (Fig. 7). Hence, to avoid any radical activity after the plasma, remaining radicals are "killed" by after-flushing with ethylene gas; which is confirmed by no observable oxidations with ethylene-treated samples. Ethylene aftertreated samples are used throughout this study.

Figures 8, 9, and 10 present IR spectra of several film and powder PPE deposits produced at different conditions at different locations. In these, a new additional peak at 800 cm^{-1} is apparent, which probably corresponds to 720 cm^{-1} peak observed in LDPE (CH_2 rock). Its intensity is strong for the first deposits (film samples) and decreases suddenly (Fig. 8) or gradually (Fig. 9). At the moment, there is no sound reason to account for these differences. However, it is important to realize at least that, for PPE, the type of product may show some structural variations with its location; and that in all samples tested in IR, the ($10.6\text{ }\mu\text{m}$) is found to be transparent.

The chemical characteristics of product are also checked by analytical means. A table is prepared for several samples tested and is presented in

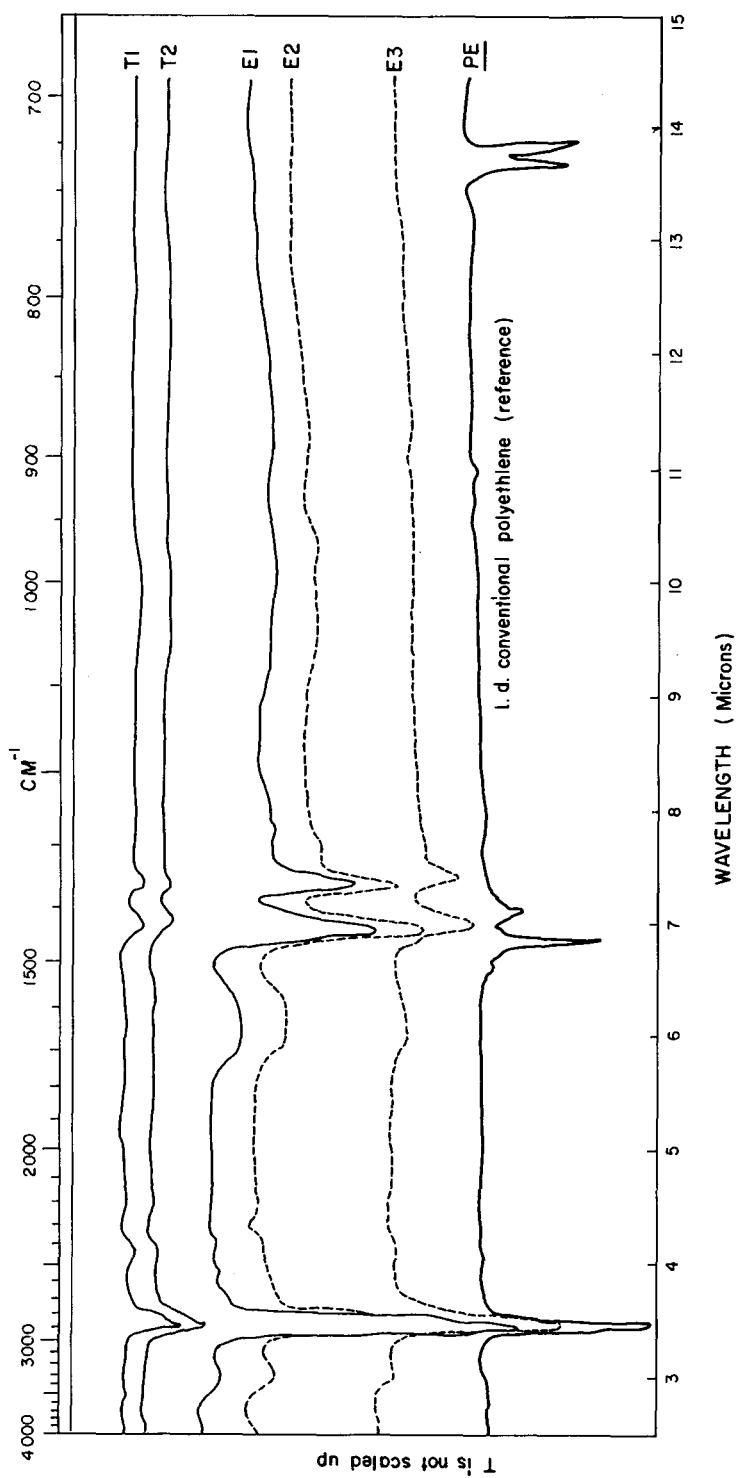


Fig. 5. IR of PPE samples as a function of location in reactor (T: sample on Teflon, E: on cooled copper electrode, all numbered beginning from entrance of reactor). Conditions: 1 Torr, 100 W, and 3.5 cc STP/min. Product is a film.

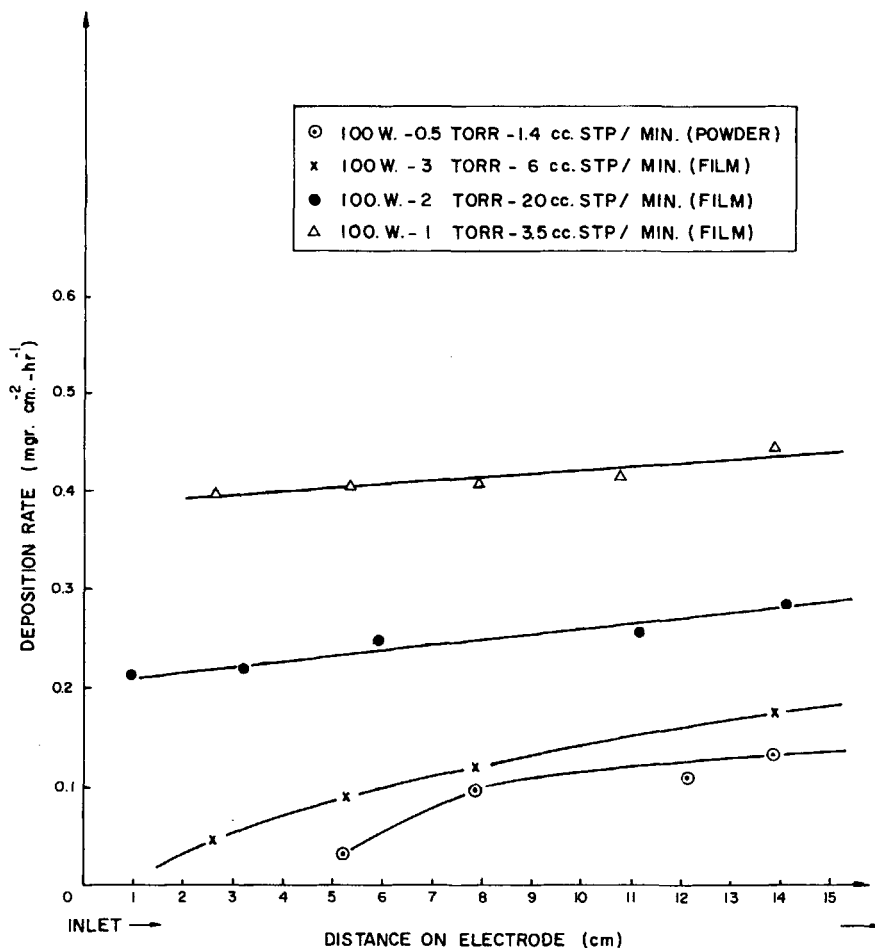


Fig. 6. Deposition profile of PPE.

(Table I). It is seen that, both the film and powdery products on cooled and hot electrodes are all "deficient" of hydrogen. This is most probably due to high extents of crosslinking, as revealed by solubility tests. Film products contain more hydrogen than powdery products. Although conditions are not exactly comparable, it seems that increase of power increases the amount of crosslinks, as expected. The rather unexpected result is the increase of (H/C) ratio for each case for the hot electrode as compared to the cold. The reason for this difference is not clear at the moment, and independent work is in progress to investigate the temperature effect; which seems to be an important parameter and is usually ignored.

Moisture-resistance studies in the humidity chamber showed that samples with up to 1 μm film coats fail after 2 hours; while for coats with 2 μm , this range is up to 10 hours. Similar tests at room humidity (50–60% RH),¹⁶ for both thicknesses led to moisture resistance for at least 100 hr. Since moisture resistance of the coat also show a strong dependency on scratches and imperfections that may exist on the virgin NaCl surface before the coat, a

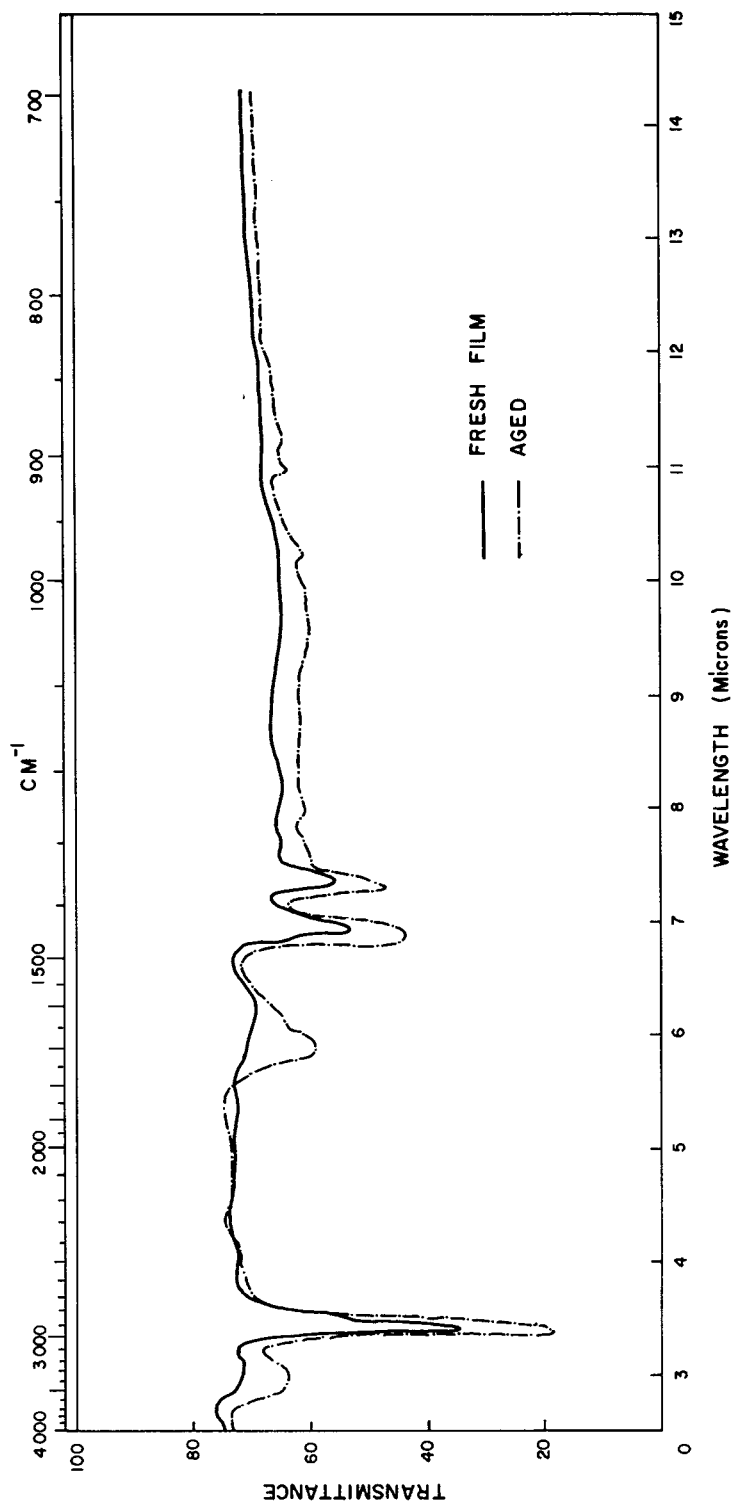


Fig. 7. IR of fresh and aged PPE films (fresh film is E2 from Fig. 5).

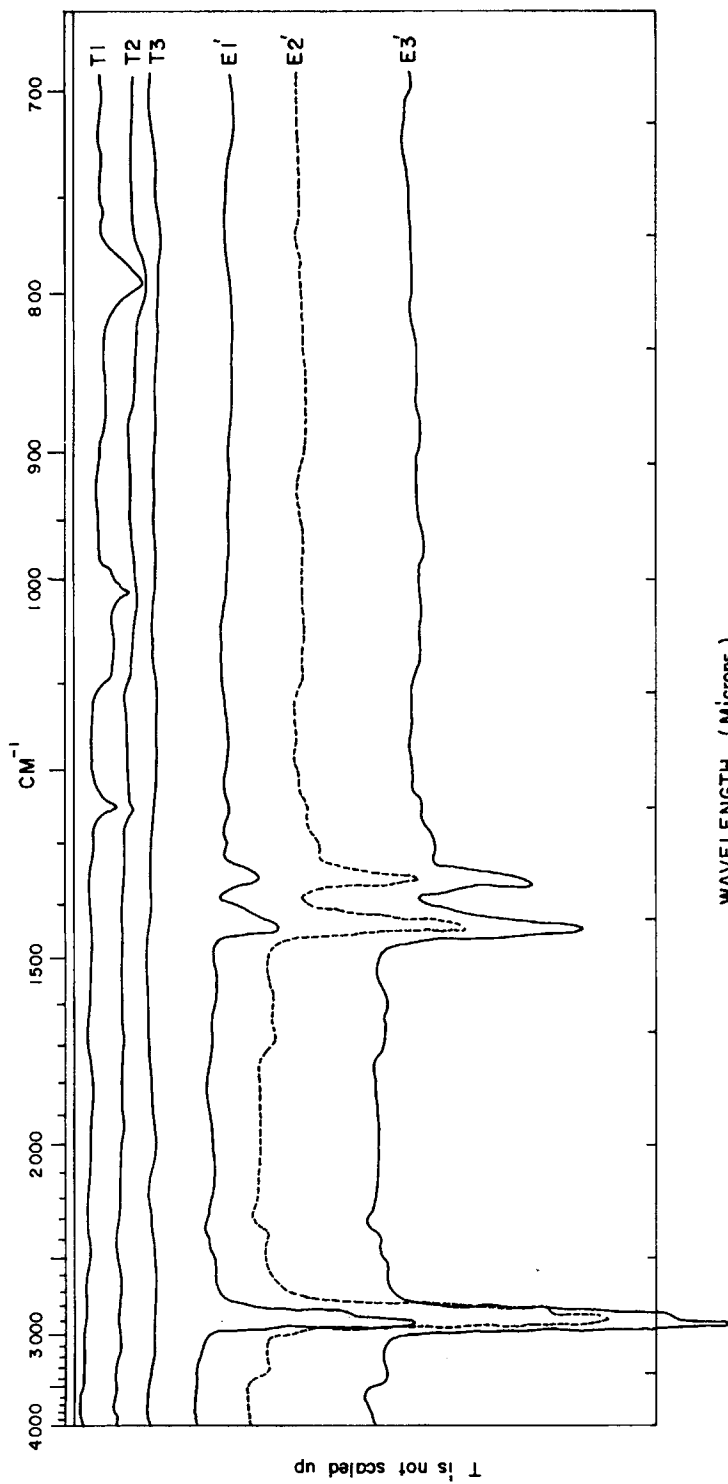


Fig. 8. IR of PPE film samples, 100 W, 3 Torr, 6 cc STP/min.

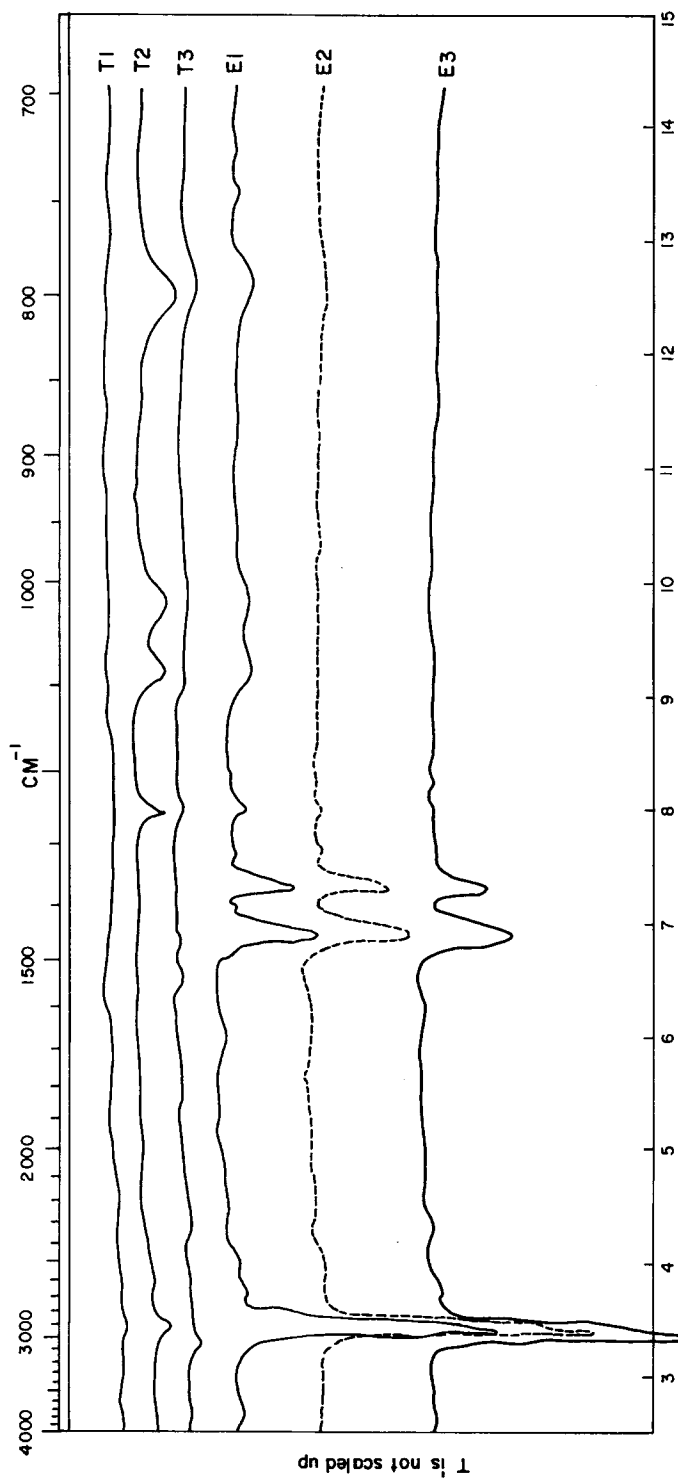
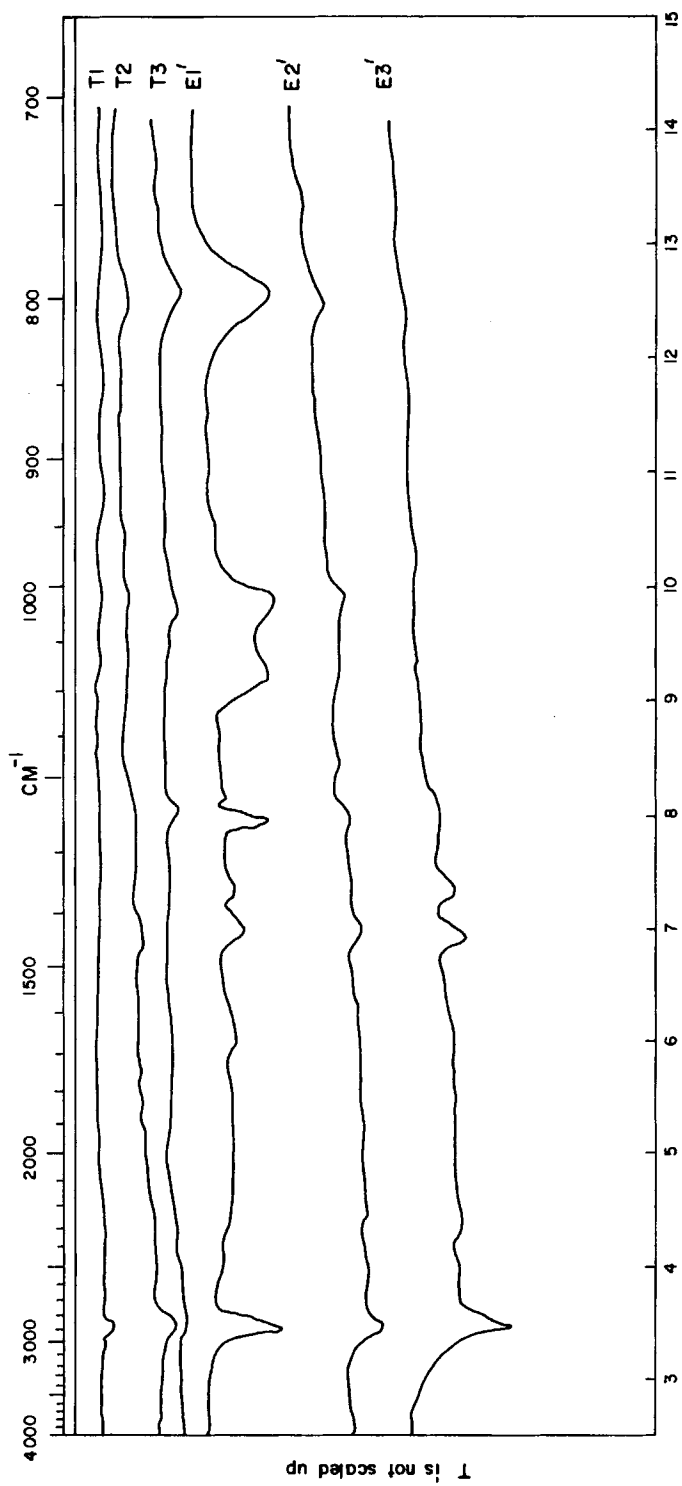


Fig. 9. IR of PPE film samples, 100 W, 2 Torr, 20 cc STP/min.



WAVELENGTH (Microns)

Fig. 10. IR of powder samples, 100 W, 1 Torr, 19.6 cc STP/min.

TABLE I
Chemical Analysis Results of Several Representative PPE Samples Produced by Plasma.

Sample no.	Reaction conditions reference (Ethane, monomer)	Physical state of product	(H)/(C) ratio of the product form	
			Cooled electrode 3.00 (ref.)	Hot electrode
1	100 W, 1 Torr (film product) 3.5 cc STP/min		1.407	—
2	75 W, 2 Torr (film product) 61.15 cc STP/min		1.581	1.896
3	50 W, 2 Torr (film product) 60.5 cc STP/min		1.737	1.979
4	100 W, 0.5 Torr (powder product) 2.11 cc STP/min		1.014	1.033

polished crystal surface for the substrate is a must for consistent results and a comparison of some polished uncoated/coated samples with each other is necessary. Both of these conditions are considered seriously in this work.

The scratch-resistance test result for sample 1 in a series of photographs are presented in (Fig. 11). Although the quality of pictures are not perfect and results are preliminary, it is clear that coat of 1 μm produce certain improvement in scratch resistance. Similar improvements are obtained for the other samples tested.

In conclusion, PPE appears as a potential protective coat for CO_2 laser NaCl window materials. Its ease of applicability as a coat with controllable homogeneous thicknesses via plasma polymerization and its transparency

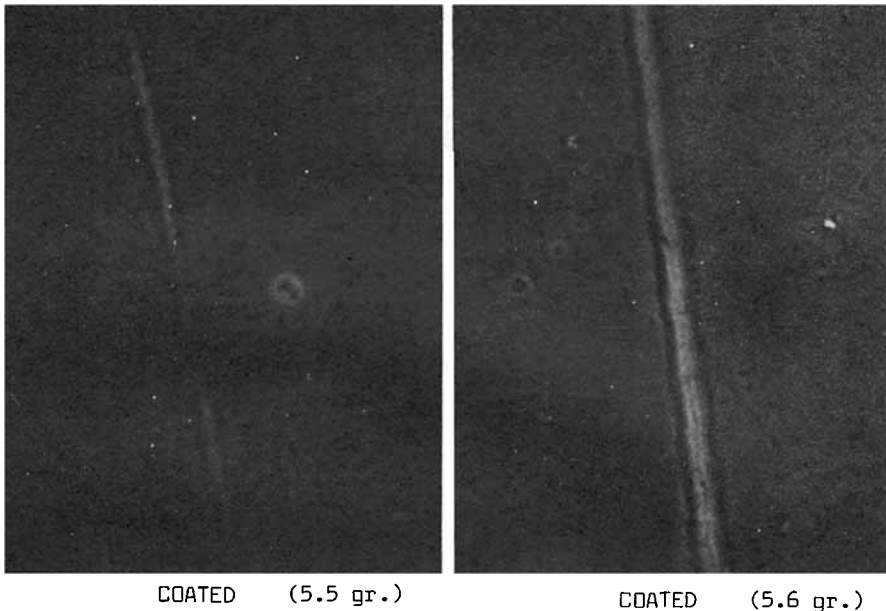


Fig. 11. A series of pictures exhibiting the scratch-resistance test results. (a) Coated, (b) Uncoated samples.

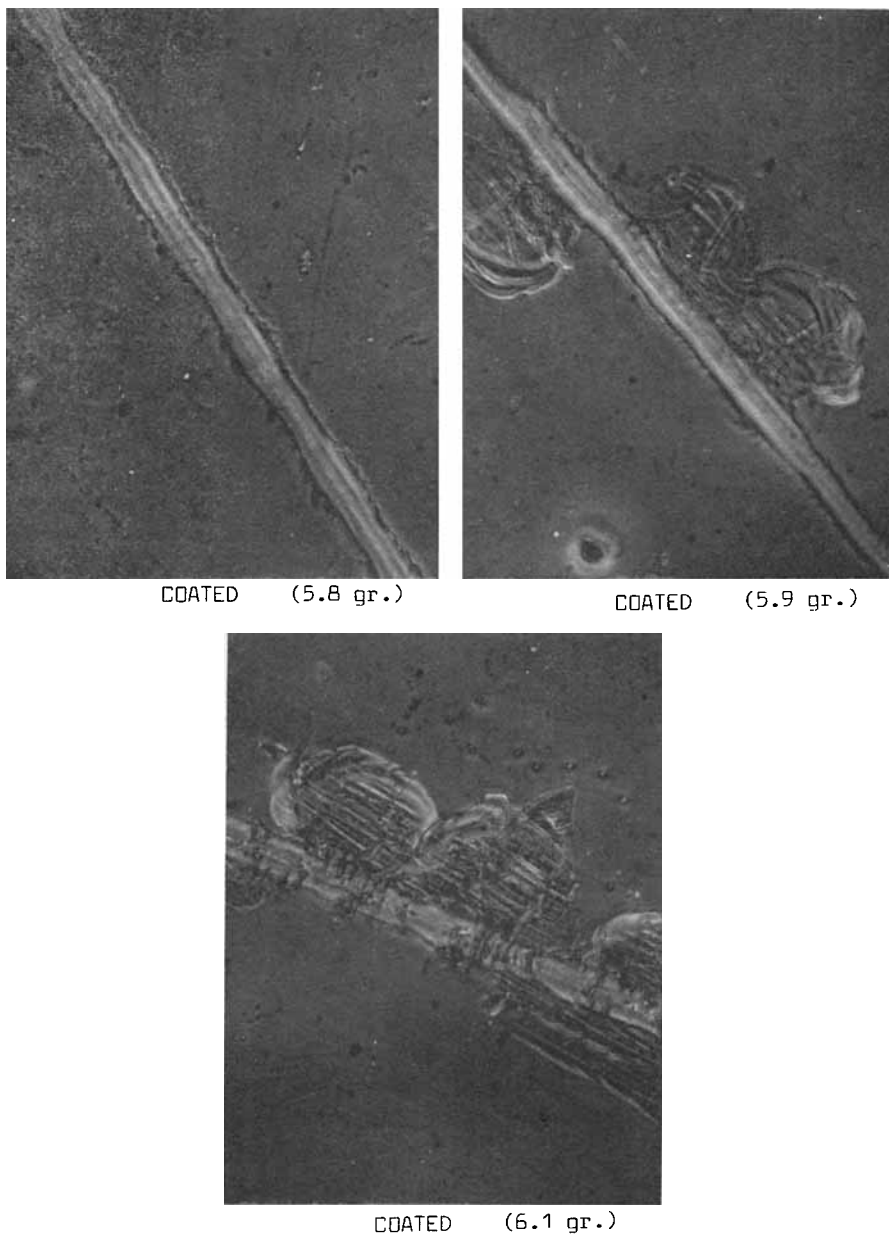


Fig. 11. (a) (Continued)

at and around $10.6 \mu\text{m}$ makes it a potential candidate. The coat shows good resistance to water-vapor permeation and its adherence to the substrate seems to be proper, and it increases scratch resistance of the substrate.

More detailed work to clarify the dependency of coat characteristics as a window material on plasma operational parameters used and substrate temperature as well as impurities is the subject of another work in progress.

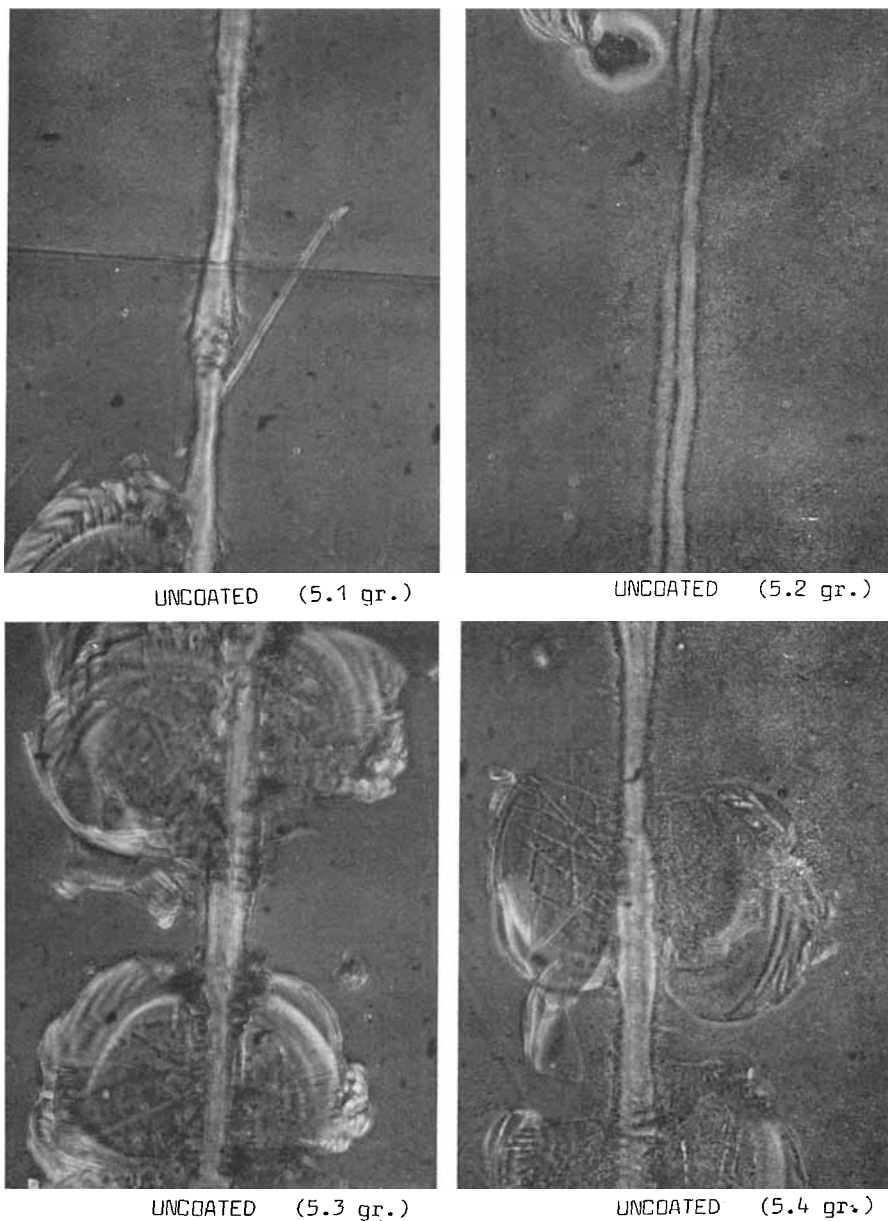


Fig. 11. (b) (Continued)

This work is supported by TUBITAK (Turkish National and Scientific Research Council), through TUMKA Unit.

References

1. M. Shen, Ed., *Plasma Chemistry of Polymers*, Marcel Dekker, New York, 1976.
2. M. Shen and A. T. Bell, Eds., *Plasma Polymerization*, A.C.S. Symposium Series. 108-ACS, Washington, D.C., 1974.

3. H. Boenig, *Plasma Science and Technology*, C. Hanser Verlag, 1983.
4. G. Akovali and G. Demirel, *J. Macromol. Sci. Chem.*, **A20.8**, 887 (1983).
5. G. Akovali and B. Orhan, *J. Polym. Sci. Polym. Chem.*, **22**, 3351 (1984).
6. G. R. Smoluk, *Mod. Plas. Int.*, **49** (May 1984).
7. H. Hiratsuka, G. Akovali, M. Shen, and A. T. Bell, *J. Appl. Polym. Sci.*, **22**, 917 (1978).
8. R. J. Jensen, A. T. Bell, and D. S. Soong, *Plasma Chem. Plasma Proc.*, **3.2.**, 139 (1983).
9. H. Kobayashi, PhD Thesis, Chem. Eng. Dept., University of California at Berkeley, 1975.
10. *CRC Handbook of Chemistry and Physics*, 56th ed., Table E46 (1976).
11. P. Benjamin and C. Weaver, *Proc. R. Ser. London*, **A254**, 177 (1960).
12. M. J. Vasile and G. Smolinsky, *J. Electrochem. Soc.*, **119**, 451 (1972).
13. L. F. Thompson and G. Smolinsky, *J. Appl. Polym. Sci.*, **16**, 1179 (1972).
14. (a) G. Akovali and M. Y. Bölük, *Polym. Eng. Sci.*, **21**(11), 658 (1981).
(b) M. Y. Bölük and G. Akovali, *Polym. Eng. Sci.*, **21**(11), 658 (1981).
15. H. Yasuda, IUPAC 3ime (Table Rande Int.), Symp. Int. de Chimie des Plasmas, Université de Limoges, France, Abstracts (1977).
16. Data presented is the lowest and highest averages reported for days of experiment as realized by Turkish Meteorological Bulletins.

Received August 28, 1985

Accepted October 2, 1985